Two-Dimensional Heterospectral Correlation Analysis of Wide-Angle X-ray Scattering and Infrared Spectroscopy for Specific Chemical Interactions in Weakly Interacting Block Copolymers

Hye Jeong Kim,[†] Seung Bin Kim,*[,‡] and Jin Kon Kim*[,†]

National Creative Research Center for Block Copolymer Self-Assembly, and Departments of Chemical Engineering and Chemistry, Pohang University of Science and Technology, Kyungbuk 790-784, Korea

Young Mee Jung*

Department of Chemistry, Kangwon National University, Chunchon 200-701, Korea

Received: June 20, 2006; In Final Form: September 1, 2006

We investigated, via two-dimensional heterospectral correlation analysis of wide-angle X-ray scattering (WAXS) and infrared (IR) spectroscopy, the specific chemical interactions existing in weakly interacting polystyrene-*block*-poly(*n*-pentyl methacrylate) copolymers (PS−PnPMA). PS−PnPMA was shown to exhibit a closed-loop-type phase behavior, where, upon heating, a lower disorder-to-order transition (LDOT) was found at lower temperatures, and an upper order-to-disorder transition (UODT) was observed at higher temperatures. The specific interaction between the PS and PnPMA blocks mainly arises from the dipole in the benzene ring of PS and the induced dipole in the PnPMA due to cluster formation with a size of 1∼2 nm. We found that the synchronous 2D WAXS−IR heterospectral correlation spectrum of the ordered state was completely different from that in the two disordered states. The CH group of the main chains of PS and PnPMA did not contribute to the cluster formation in the two disordered states, indicating that the main chains of PS and PnPMA blocks were randomly distributed in the two disordered states. However, only the C═C group in the PS block contributed to the cluster at a disordered state below the LDOT, whereas both the C−C−O group in PnPMA and the entire phenyl ring and C═C group in PS contributed to cluster formation at another disordered state above the UODT. Thus, the probability that PS (and PnPMA) chains were located at their own neighboring chains at one disordered state above the UODT is larger than that at another disordered state below the LDOT.

1. Introduction

Generalized two-dimensional (2D) correlation spectroscopy is a well-established technique that provides considerable utility and benefit in various spectroscopic studies of polymers.[1−7] Some of the important features of generalized 2D correlation spectra are simplification of complex spectra consisting of many overlapped peaks, enhancement of spectral resolution by spreading peaks along the second dimension, establishment of unambiguous assignments through the correlation of bands selectively coupled by various interaction mechanisms, and determination of the sequence of the spectral peak emergence.

A very intriguing method in 2D correlation spectroscopy is 2D *heterospectral correlation analysis*, where two completely different types of spectra for a system obtained by using multiple spectroscopic probes under the same external perturbation are compared.[8−14] From the response patterns of the system monitored by two different probes under the same perturbation, one could detect a correlation between two spectral signals. For instance, 2D heterospectral correlation analysis between closely related spectroscopic measurements,[9,10,12,14] such as infrared (IR) and Raman spectra, which are very attractive from the point of better understanding its complementary vibration spectra, provides especially rich insight and clarification into the in-depth study of vibrational spectra. The 2D heterospectral correlation spectroscopy has been applied to small-angle X-ray scattering (SAXS) and IR spectra of a dynamically strained block copolymer film.[8] The molecular-level orientational dynamics of polymer chain segments probed by IR spectroscopy was directly correlated to the structural reorganization of the supermolecular structure of the microphase-separated specimen monitored by the change in the scattering pattern of the X-ray.

Recently, we have reported, by using SAXS, rheometry, and depolarized light scattering, that the polystyrene-*block*-poly(*n*-pentyl methacrylate) copolymer (PS−PnPMA) exhibited a closed-loop phase behavior bounded by the lower disorder-to-order transition (LDOT) and the upper order-to-disorder transition (UODT).[15−21] However, the exact mechanism of the closed-loop-type phase behavior of PS−PnPMA is not yet known. To understand this mechanism based on the molecular level of each chain, we employed the temperature-dependent Fourier transform infrared (FTIR) spectra of PS−PnPMA and showed that the transition temperatures and phase behavior of PS−PnPMA were determined by spectroscopic studies.[6,7] For weakly interacting polymer systems, the origin of the LDOT (or the lower critical solution transition (LCST)) might be 2-fold.[22−28] The first is a free volume effect arising from the difference in

* To whom correspondence should be addressed. E-mail: jkkim@postech.ac.kr (J.K.K.); sbkim@postech.ac.kr (S.B.K.); and ymjung@kwangwon.ac.kr (Y.M.J.).

[†] National Creative Research Center for Block Copolymer Self-Assembly, and Department of Chemical Engineering.

[‡] Department of Chemistry.

10.1021/jp0638282 CCC: $33.50
Published on Web 10/20/2006

compressibilities of the two components (or the equation-of-state variables). In this situation, with increasing temperature, the degree of phase-separation increases because of the increased free volume effect. The second is related to the directional entropy. At lower temperatures, a weak favorable interaction, though small, can surpass the directional entropic loss resulting from pairing two monomers. But, the directional entropic loss becomes large with increasing temperature, which results in the LDOT (or LCST).

The weak interactions in PS−PnPMA could arise from the interaction between the dipole in the phenyl ring and the induced dipole in the PnPMA block. The induced dipole could be expected for the hindered chain motion of the rigid group, such as the cyclohexyl group in poly(cyclohexyl acrylate) (PCHA). It is noted that PS/PCHA blends showed LCST-type phase behavior due to the specific interaction.[29] Although PnPMA chains do not seem to have any rigid group, Beiner et al. showed, via wide-angle X-ray scattering (WAXS), that the alkyl group in poly(*n*-alkyl acrylate) (PnAA) or poly(*n*-alkyl methacrylate) (PnAMA) forms clusters (or nanophase domains) with sizes of 0.5∼2 nm depending upon the length of the alkyl group.[30,31] Once the *n*-pentyl group in the PnPMA chains of PS−PnPMA forms clusters, it could contribute to the hindered chain motion of PnPMA. This indicates that a specific interaction, although weak, could exist between PS and PnPMA blocks. However, the WAXS itself could not give detailed information, for instance, which groups of PS−PnPMA contribute to the clusters. This led us to consider the 2D WAXS−IR heterospectral correlation spectroscopy, from which we could understand the detailed mechanism of the clusters and the weak interaction in PS−PnPMA.

In the present study, we have performed 2D correlation spectroscopy of IR spectroscopy as well as 2D WAXS−IR heterospectral correlation spectroscopy to investigate in detail the phase behavior of PS−PnPMA. The 2D WAXS−IR heterospectral correlation analysis has not yet been investigated for any polymer blend or block copolymer. We showed that the synchronous 2D hetero correlation spectrum of the ordered state was completely different from that in the two disordered states. The CH group of the main chains of PS and PnPMA did not contribute to the cluster formation in the two disordered states, indicating that the main chains of PS and PnPMA blocks were uniformly distributed at two disordered states. However, we showed that only the C═C group in the PS block contributed to the cluster with a size of 1−2 nm at a disordered state below the LDOT, whereas both the C−C−O group in PnPMA and the phenyl ring and C═C group in PS contributed to the cluster formation at another disordered state above the UODT. Thus, the probability that PS (or PnPMA) chains were located at their own neighboring chains in one disordered state above the UODT is larger than that in another disordered state below the LDOT.

2. Experimental Section

PS−PnPMA was synthesized by the sequential, anionic polymerization of styrene and *n*-pentyl methacrylate in tetrahydrofuran at −78 °C under purified argon by using *sec*-BuLi as an initiator. The number and weight average molecular weights (M_n and M_w) of PS−PnPMA were determined (49 000 and 49 900 g mol^{-1}) by size exclusion chromatography coupled with a multiangle laser light scattering detector.[15,16] The volume fraction of the PS block was 0.5. PS−PnPMA and showed two transition temperatures (LDOT and UODT) at 140 °C and 224 °C, as determined by SAXS, rheometry, and depolarized light scattering.

Synchrotron WAXS profiles ($I(q)$ vs $q(= 4\pi \sin\theta/\lambda)$, where q is the scattering vector, 2θ is the scattering angle, and λ is the wavelength) were conducted at the 4C2 beamline at the Pohang Light Source (PLS), Korea. A one-dimensional position-sensitive detector (Diode-Array PSD; Princeton Instruments, Inc.; model ST-120) with a distance of each diode of 25 μm was used. The sample thickness was 1 mm, and the sample-to-detector distance was 0.5 m. The exposure time was 5 s. The sample was first annealed at 120 °C for 2 days to remove any thermal history. Then the WAXS profiles were obtained at various temperatures from 120 °C to 260 °C at intervals of 10 °C after the sample was equilibrated for 30 min at the measurement temperature.

FTIR spectra were measured at a spectral resolution of 4 cm^{-1} with a Bomem DA8 FTIR spectrometer equipped with a liquid nitrogen-cooled MCT detector. The Seagull attachment (Harrick Scientific Corporation), which includes a heating block attachment, was used in this study. A powder consisting of PS−PnPMA and KBr was prepared by using a freezer mill. Before the powder was made, PS−PnPMA was annealed at 120 °C for 2 days. All diffuse reflectance FTIR spectra were measured by co-adding 256 scans from 120 to 260 °C at intervals of 10 °C after the sample was equilibrated for 30 min at the measurement temperature. Baseline correction was performed for all diffuse reflectance FTIR spectra before calculation of the 2D correlation spectra. Synchronous 2D correlation spectra were obtained by using the same software described previously.[6]

3. Results and Discussion

Figure 1 a,b shows the FTIR spectra for PS−PnPMA obtained during heating from 120 to 260 °C in the regions of 1000−2000 cm^{-1} and 2700−3200 cm^{-1} focusing on the side chain groups and the main chain groups (CH stretching modes), respectively. The band assignments of PS−PnPMA are given in Table 1.[2,6−8,32] Interestingly, the intensity of the C−C−O mode at 1255 cm^{-1} was greater than that at 1274 cm^{-1} at lower temperatures, whereas the opposite was observed at higher temperatures. This indicates that the conformation of the PnPMA is different in the two temperature regions.[6,7]

To understand in detail the closed-loop phase behavior, we performed 2D correlation analysis. As reported in our previous paper,[6] 2D correlation spectroscopy is a well-established technique for interpreting spectral data sets obtained during the observation of spectra with an external perturbation. The intensity of a 2D correlation spectrum $X(\nu_1, \nu_2)$ is expressed by the dynamic spectrum of a system ($\tilde{y}(\nu,t)$) as follows:

$$X(\nu_1,\nu_2) = <\tilde{y}(\nu_1,t)\tilde{y}(\nu_2,t')> \quad (1)$$

$$\tilde{y}(\nu,t) = y(\nu,t) - \bar{y}(\nu) \quad (2)$$

Here, $y(\nu,t)$ is the perturbation-induced variation of a spectral intensity measured at a spectral variable along the external perturbation t (e.g., temperature in this study) between T_{max} and T_{min}, and $\bar{y}(\nu)$ is the reference spectrum chosen as the averaged spectrum. To simplify the mathematical manipulation, $X(\nu_1, \nu_2)$ is treated as a complex number function consisting of two orthogonal (i.e., real and imaginary) components, known as the synchronous (Φ) and asynchronous (Ψ) 2D correlation intensities, respectively:

$$X(\nu_1,\nu_2) = \Phi(\nu_1,\nu_2) + i\Psi(\nu_1,\nu_2) = \frac{1}{\pi(T_{max} - T_{min})}\int_0^\infty \tilde{Y}(\nu_1,\omega) \cdot \tilde{Y}^*(\nu_2,\omega)\mathrm{d}\omega \quad (3)$$

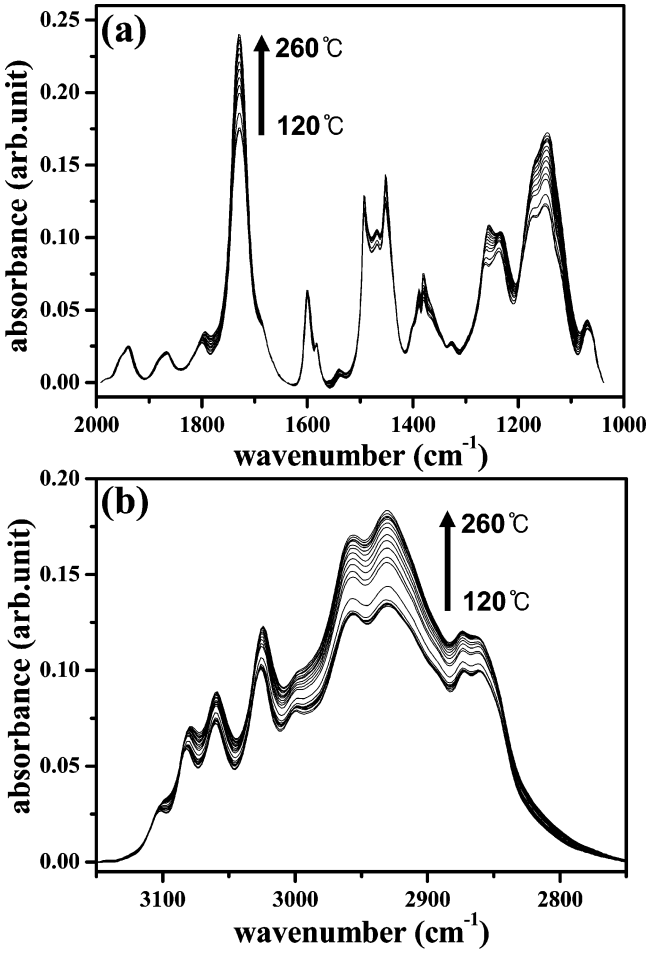

Figure 1. FTIR spectra for PS−PnPMA obtained during heating from 120 to 260 °C at intervals of 10 °C in two wavelength regions: (a) 1000−2000 cm^{-1} focusing on the side groups and (b) 2700−3200 cm^{-1} focusing on the C−H stretching for the main chains in PS−PnPMA.

TABLE 1. Assignments for Bands of PS−PnPMA[a]

wavenumber (cm^{-1})	assignments
3060	aromatic C−H stretching mode
2957	CH_3 symmetric stretching mode in PnPMA block
2931	CH_2 asymmetric stretching mode in PS block
1731	C═O stretching mode
1500−1600	C═C stretching modes in the PS block
1452, 1492	phenyl ring stretching modes
1382, 1391	C−H deformation modes
1274, 1255	C−C−O stretching modes
1140	C−O stretching mode

[a] Mode description of PS in PS−PnPMA is adapted from the model compound of monosubstituted benzenes.[32] No band in PnPMA appears in the region of 1500−1600 cm^{-1}. Vibrations in this region mainly involve "quadrant stretching" of the phenyl ring C═C bonds, but there is a little interaction with CH in-plane bending.

in which $\tilde{Y}$ and $\tilde{Y}^*$ are the Fourier transform and the conjugate of the Fourier transform of $\tilde{y}(\nu,t)$, respectively. The intensity of the peaks located at the diagonal positions in the synchronous 2D spectrum represents the overall susceptibility of the corresponding spectral region to change in spectral intensity as an external perturbation is applied to the system. Cross-peaks located at the off-diagonal positions of a synchronous 2D spectrum represent simultaneous or coincidental changes of spectral intensities observed at two different spectral variables (ν_1 and ν_2). From 2D correlation spectra, we can get information on the molecular environment among the chains.

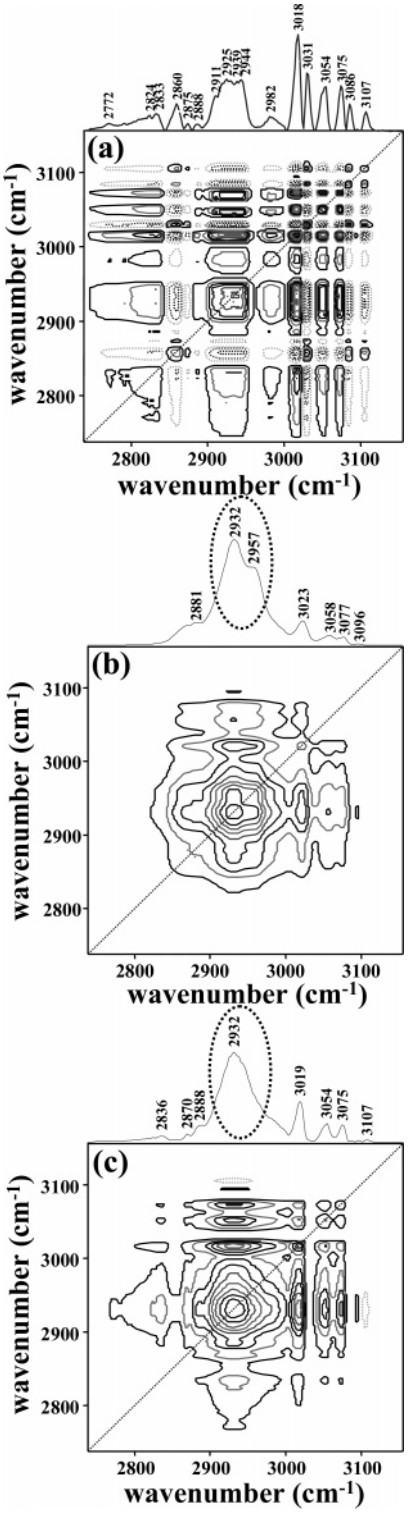

Figure 2. Synchronous 2D correlation spectra in the region 2700−3200 cm^{-1} focusing on the C−H stretching at three different temperature regions: (a) a disordered state below the LDOT (120−140 °C), (b) an order state (150−200 °C), and (c) another disordered state above the UODT (220−260 °C). Solid and dashed lines in the spectra represent positive and negative cross-peaks, respectively.

Figure 2a−c shows synchronous 2D correlation spectra in the region 2700−3200 cm^{-1}, focusing on the C−H stretching of the main chains (PS and PnPMA) at three different regimes: a lower disordered state, an ordered state, and a higher disordered state, respectively. It is noted that Figure 2 was constructed from Figure 1b and eqs 1−3. The 2D correlation spectrum for a disordered state at lower temperature is distinctly

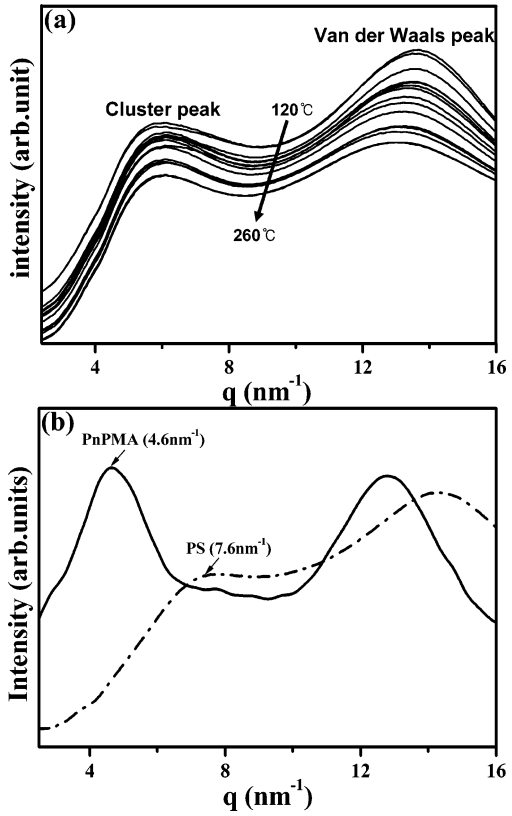

Figure 3. WAXS profiles of (a) PS−PnPMA obtained during heating from 120 to 260 °C at intervals of 10 °C and (b) PS and PnPMA homopolymers measured at 25 °C.

different from that for another disordered state at higher temperature. Power spectra extracted along the diagonal line of the synchronous spectra are shown in the top of Figure 2. Interestingly, the power spectrum of the 2D correlation spectrum for a disordered state at higher temperature seems to be more similar to that for an ordered state compared with another disordered state at lower temperatures. This means that the probability that PS (or PnPMA) chains are located at their own neighboring PS (or PnPMA) chains in the disordered state at higher temperatures was larger than that in another at lower temperatures. This result indicates that two disordered states have different neighboring environments, consistent with results reported in our previous study.[6,7]

Figure 3a shows the change in the WAXS intensity profile of PS−PnPMA with temperature upon heating from 120 to 260 °C. Interestingly, PS−PnPMA exhibited both a cluster peak located at ∼6 nm^{-1} and a van der Waals peak located at ∼13.6 nm^{-1} at all measuring temperatures. It is seen in Figure 3b that the cluster peak in PS−PnPMA is located between the cluster peaks for PnPMA homopolymer (4.6 nm^{-1}) and PS homopolymer (7.6 nm^{-1}). The smaller size (or larger q value) for the cluster peak in PS−PnPMA compared with that of PnPMA homopolymer is due to the presence of PS chains in PS−PnPMA. Previously, Beiner et al. reported, via WAXS and relaxation spectroscopy, that alkyl groups of PnAA and PnAMA homopolymers formed clusters (or nanodomains) with a size of 0.5−2 nm depending on the carbon number of alkyl groups. The existence of the cluster is very important in that it could give a source of the induced dipole in PnPMA. It is noted that the induced dipole of the PnPMA block is expected for the hindered motion arising from the clusters. Once the induced dipole exists, the favorable specific interaction between PS and PnPMA blocks is expected because of the dipole in PS and the induced dipole interaction. However, WAXS profiles alone do not give any information as to which functional groups contribute to the cluster formation.

Therefore, we introduced the 2D heterospectral correlation analysis between WAXS and FTIR spectra based on Figures 1 and 3. The 2D heterospectral correlation analysis is to compare one dynamic spectrum $\tilde{y}(\nu,t)$ measured by one technique (e.g., FTIR absorbance) with another dynamic spectrum $\tilde{z}(\mu,t)$ measured with a completely different probe (e.g., X-ray scattering profile). The general form of the heterospectral 2D correlation is given by

$$X(\nu,\mu) = <\tilde{y}(\nu,t)\tilde{z}(\mu,t')> \quad (4)$$

and the synchronous ($\Phi(\nu,\mu)$) and asynchronous ($\Psi(\nu,\mu)$) heterospectral correlation spectrum is obtained from

$$X(\nu,\mu) = \Phi(\nu,\mu) + i\Psi(\nu,\mu) = \frac{1}{\pi(T_{max} - T_{min})}\int_0^\infty \tilde{Y}(\omega)\cdot\tilde{Z}^*(\omega)d\omega \quad (5)$$

in which $\tilde{Y}$ and $\tilde{Z}^*$ are the Fourier transform and the conjugate of the Fourier transform of $\tilde{y}(\nu,t)$ and $\tilde{z}(\nu,t)$, respectively.

Figure 4a−c shows the synchronous 2D heterospectral correlation analysis between WAXS and FTIR spectra for PS−PnPMA at three temperature regimes. When the cross-peak in the heterospectral analysis is positive, the cluster peak in the WAXS profile is directly correlated to the specific IR band. If the cross-peak becomes negative, the cluster peak does not have any correlation to the IR band.[2] It is seen in Figure 4 that the synchronous 2D heterospectral correlation spectrum in the ordered state is completely different from those in the two disordered states. Specifically, the cluster peak at ∼6 nm^{-1} in the ordered state is strongly correlated with all the functional groups (or bands) corresponding to 1000−1800 cm^{-1}. This is because of the microdomain structures of PnPMA block in the ordered state. It is also seen that the band for the C═C stretching mode of the phenyl ring (∼1602 cm^{-1}) in the PS block becomes a positive correlation with WAXS profiles for all three temperature regimes. Very interestingly, a disordered state at higher temperatures, a band at 1274 cm^{-1} corresponding to the C−C−O stretching mode, and a band at 1452 and 1492 cm^{-1} corresponding to the phenyl ring stretching mode as well as the C═C stretching mode in the PS block become positive correlations with the cluster peak, whereas these two peaks except for C═C stretching modes (∼1550 and 1602 cm^{-1}) in the PS block in another disordered state at lower temperatures did not have any correlation with the cluster peak. Another interesting thing in Figure 4c is that the change in the cluster peak for C−C−O groups (∼ 1275 and ∼ 1450 cm^{-1}) with temperature in the disordered state at higher temperature showed tiny maxima at two values of q at ∼4.0 and 7.5 nm^{-1} *rather than* ∼6 nm^{-1}. It is noted that the intensity itself of the cluster peak in this disordered region is the largest at $q \sim 6$ nm^{-1}, as shown in Figure 3a. Since these two q values (∼4.0 and 7.5 nm^{-1}) are close to the peak positions for PnPMA and PS homopolymers (see Figure 3b), we consider that the probability that PS (or PnPMA) chains are located at their own neighboring PS (or PnPMA) chains in the disordered state at higher temperature is larger than that in another at lower temperature. From Figures 2 and 4, we consider that the side chains of PS and PnPMA in a lower disordered state are more randomly distributed than those in another disordered state at high temperatures. Since the favorable specific interaction mainly arises between the C−C−O and the phenyl ring, the degree of

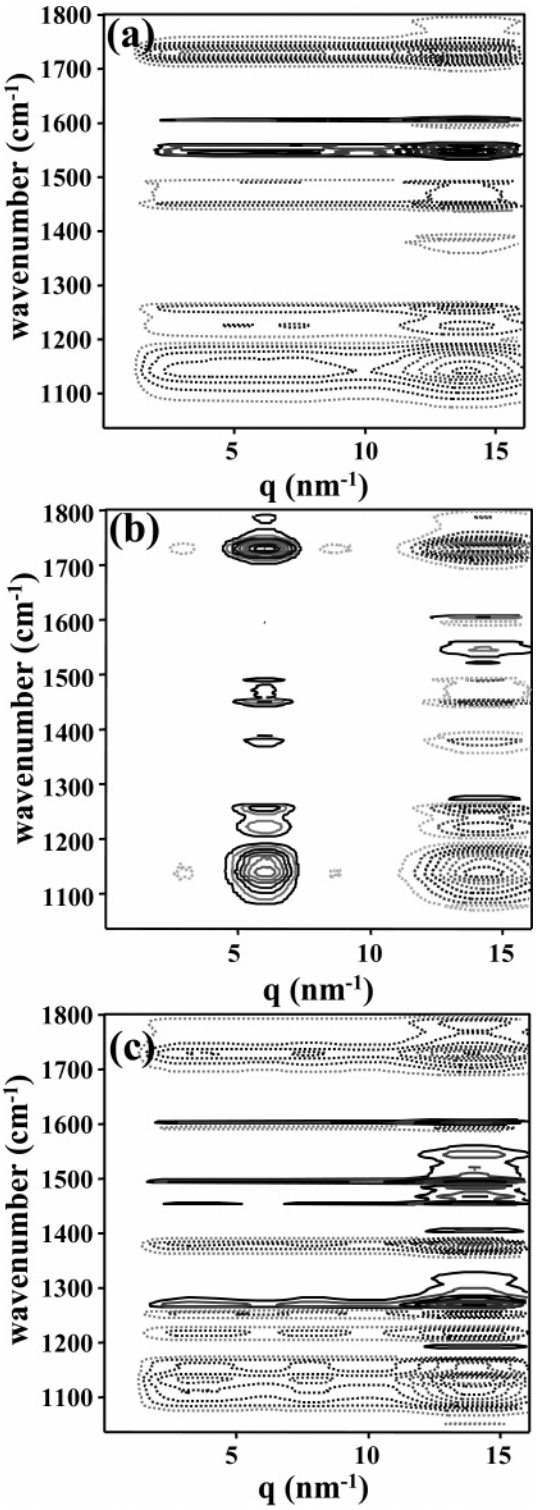

Figure 4. Synchronous 2D heterospectral correlation analysis between WAXS and FTIR spectra in 1000−1800 cm^{-1} focusing on the side groups for PS−PnPMA at three different temperature regimes: (a) a disordered state below the LDOT (120−140 °C), (b) an ordered state (150−200 °C), and (c) another disordered state above the UODT (220−260 °C). Solid and dashed lines in the spectra represent positive and negative cross-peaks, respectively.

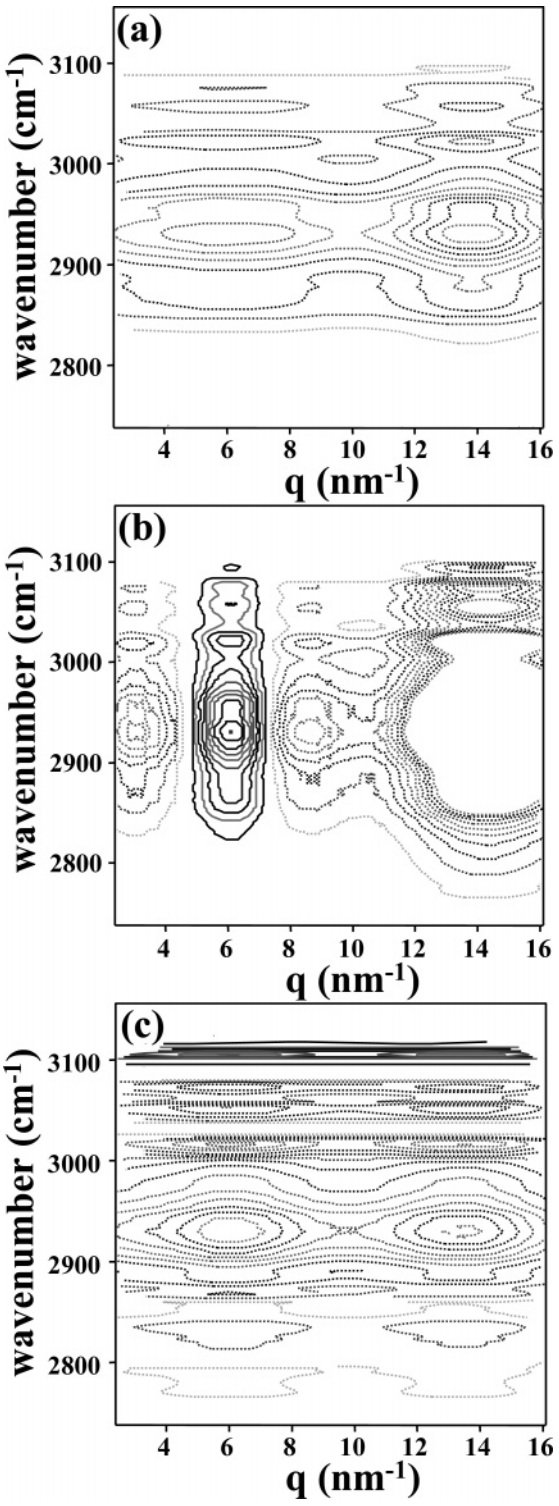

Figure 5. Synchronous 2D heterospectral correlation analysis between WAXS and FTIR spectra in 2700−3200 cm^{-1} focusing on the C−H stretching in the main chains for PS−PnPMA at three different temperature regimes: (a) a disordered state below the LDOT (120−140 °C), (b) an ordered state (150−200 °C), and (c) another disordered state above the UODT (220−260 °C). Solid and dashed lines in the spectra represent positive and negative cross-peaks, respectively.

the specific interaction at a lower disordered state would be larger than that at a higher disordered state.

Figure 5a−c shows synchronous 2D heterospectral correlation spectra of the CH stretching of the main chains (PS and PnPMA) at three temperature regimes. The cluster peak showed negative correlation to the bands belonging to the main chains in both of the two disordered states, suggesting that the cluster formation in these two regimes is not due to the main chain. On the basis of the above results, we can give a schematic describing three different morphological states of PS−PnPMA, as given in Figure 6. A disordered state at lower temperatures is different from that at higher temperatures. Namely, the main chain might be randomly distributed at both of the two disordered states,

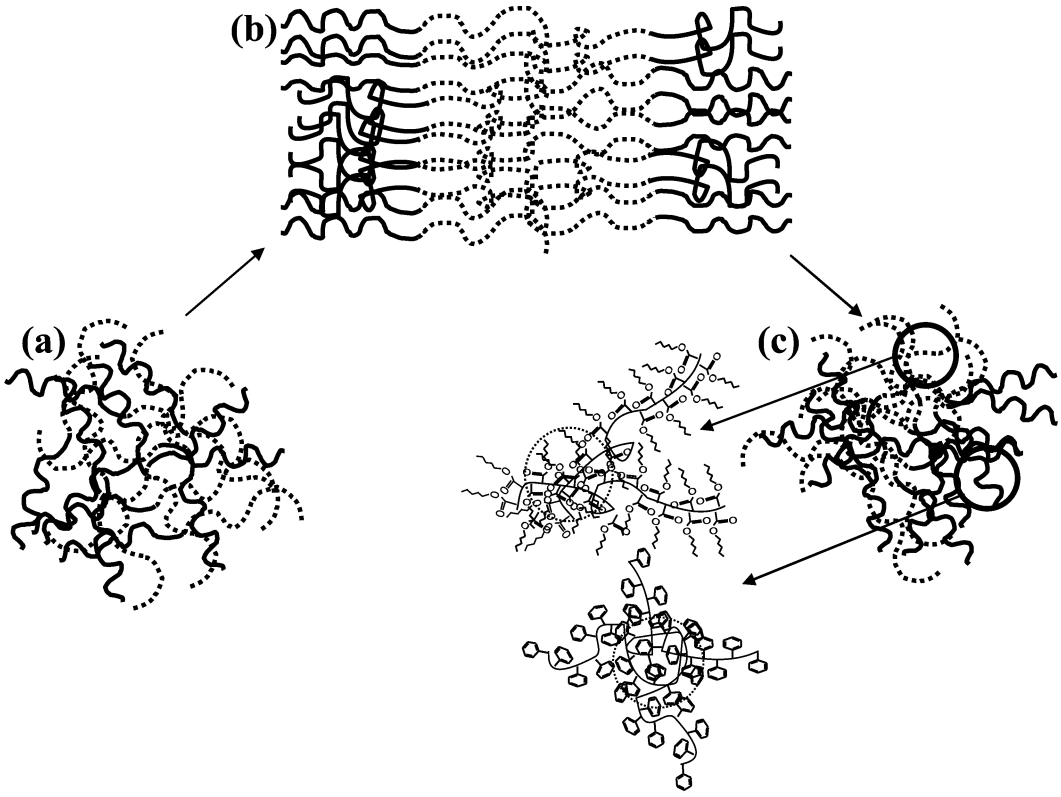

Figure 6. Schematic for the chain distributions of PS and PnPMA at three temperature regimes: (a) a disordered state below the LDOT, (b) an ordered state, and (c) another disordered state above the UODT. Solid and dashed lines represent the PS block and the PnPMA block, respectively.

whereas the side chains of PS (and PnPMA) in a disordered state at higher temperatures are located at their own neighboring PS (and PnPMA) chains compared with those at a lower disordered state. This indicates that the specific interaction at a lower disordered state might be stronger than that at another disordered state at higher temperatures. This is also consistent with our previous SAXS results[15] that the SAXS intensity at a lower disordered state is smaller than that of a higher disordered state, although both are much smaller than the SAXS intensity at an ordered state. Therefore, we consider that the disordered state at lower temperatures mainly arises from the relatively strong favorable interaction between the C−C−O group and the phenyl ring via induced dipole−dipole interaction, whereas the disordered state at higher temperatures is mainly due to the strong increase in the combinatorial entropy, although a small interaction still exists.

4. Conclusions

We have shown that 2D heterospectral correlation analysis of WAXS and IR spectroscopy is very useful in the characterization of the specific chemical interactions existing in weakly interacting PS−PnPMA. The interaction between the PS and PnPMA blocks is mainly due to the dipole in the phenyl ring of PS and the induced dipole of PnPMA resulting from the formation of a cluster with a size of 1−2 nm. The synchronous 2D WAXS−IR heterospectral correlation spectrum of PS−PnPMA in the ordered state was completely different from that in the two disordered states. The CH group of the main chains of PS and PnPMA did not contribute to the cluster formation in the two disordered states, indicating that the main chains of PS and PnPMA blocks were uniformly distributed at the two disordered states. However, we have shown that only the C═C group in the PS block contributed to the cluster with a size of 1−2 nm at a disordered state below the LDOT, whereas both the C−C−O group in the PnPMA block and the entire phenyl ring and C═C group in PS contributed to the cluster formation at another disordered state above the UODT. Thus, the probability that PS (and PnPMA) chains were located at their own neighboring PS (and PnPMA) chains in one disordered state above the UODT is much higher than that in another disordered state below the LDOT. These results led us to conclude that the disordered state at lower temperatures mainly arises from the relatively strong favorable interaction, whereas the disordered state at higher temperatures is mainly due to the strong increase in the combinatorial entropy, although a tiny favorable interaction still exists.

Acknowledgment. This work was supported by the Creative Research Initiative Program by the Korea Organization of Science and Engineering Foundation (KOSEF), the Second Stage of Brain Korea 21 Project, and a Korea Research Foundation Grant funded by the Korean Government (MOE-HRD) (KRF-2005-204-C00031). WAXS was performed at the PLS beam line supported by the Pohang Iron & Steal Co., Ltd. (POSCO) and KOSEF.

References and Notes

(1) Noda, I.; Dowrey, A. E.; Marcott, C.; Story, G. M.; Ozaki, Y. *Appl. Spectrosc.* **2000**, *54*, 236A.

(2) Noda, I.; Ozaki, Y. *Two-Dimensional Correlation Spectroscopy: Applications in Vibrational Spectroscopy*; John Wiley & Sons: New York, 2004.

(3) Ozaki, Y.; Liu, Y.; Noda, I. *Macromolecules* **1997**, *30*, 2391.

(4) Shin, H. S.; Jung, Y. M.; Lee, J.; Chang, T.; Ozaki, Y.; Kim, S. B. *Langmuir* **2002**, *18*, 5523.

(5) Jung, Y. M.; Shin, H. S.; Czarnik-Matusewicz, B.; Noda, I.; Kim, S. B. *Appl. Spectrosc.* **2002**, *56*, 1568.

(6) Kim, H. J.; Kim, S. B.; Kim, J. K.; Jung, Y. M.; Ryu, D. Y.; Lavery, K. A.; Russell, T. P. *Macromolecules* **2006**, *39*, 408.

(7) Jung, Y. M.; Kim, H. J.; Ryu, D. Y.; Kim, S. B.; Kim, J. K. *J. Mol. Struct.*, in press.

(8) Noda, I. *Chemtract−Macromol. Chem*. **1990**, *1*, 89.
(9) Czarnecki, M. A.; Wu, P.; Siesler, H. W. *Chem. Phys. Lett.*. **1998**, *283*, 326.
(10) Jung, Y. M.; Czarnik-Matusewicz, B.; Ozaki, Y. *J. Phys. Chem. B* **2000**, *104*, 7812.
(11) Nagai, N.; Yamaguchi, Y.; Saito, R.; Hayashi, S.; Kudo, M. *Appl. Spectrosc.* **2001**, *55*, 1207.
(12) Awichi, A.; Tee, E. M.; Srikanthan, G.; Zhao, W. *Appl. Spectrosc.* **2002**, *56*, 897.
(13) Choi, H. C.; Jung, Y. M.; Noda, I.; Kim, S. B. *J. Phys. Chem. B* **2003**, *107*, 5806.
(14) Schultz, G.; Jirasek, A.; Blades, M. W.; Turner, R. F. B. *Appl. Spectrosc.* **2003**, *57*, 156.
(15) Ryu, D. Y.; Jeong, U.; Kim, J. K.; Russell, T. P. *Nat. Mater*. **2002**, *1*, 114.
(16) Ryu, D. Y.; Jeong, U.; Lee, D. H.; Kim, J.; Youn, H. S.; Kim, J. K. *Macromolecules* **2003**, *36*, 2894.
(17) Ryu, D. Y.; Park, M. S.; Chae, S. H.; Jang, J.; Kim, J. K.; Russell, T. P. *Macromolecules* **2002**, *35*, 8676.
(18) Ryu, D. Y.; Lee, D. J.; Kim, J. K.; Lavery, K. A.; Russell, T. P.; Han, Y. S.; Sung, B. S.; Lee, C. H.; Thiyagarajan, P. *Phys. Rev. Lett.* **2003**, *90*, 235501.
(19) Ryu, D. Y.; Lee, D. H.; Jeong, U.; Yun, S. H.; Park, S.; Kwon, K.; Sohn, B. H.; Chang, T.; Kim, J. K.; Russell, T. P. *Macromolecules* **2004**, *37*, 3717.
(20) Ryu, D. Y.; Lee, D. H.; Jang, J.; Kim, J. K.; Lavery, K. A.; Russell, T. P. *Macromolecules* **2004**, *37*, 5851.
(21) Kim, J. K.; Jang, J.; Lee, D. H.; Ryu, D. Y. *Macromolecules* **2004**, *37*, 8599.
(22) Sanchez, I. C.; Panayiotou, C. G. In *Models for Thermodynamic and Phase Equilibria Calculation*; Sandler, S. I., Ed.; Marcel Dekker, Inc: New York, 1994.
(23) Prausnitz, J. M.; Lichtenthaler, R. N.; Gomes de Azevedo, E. *Molecular Thermodynamics of Fluid-Phase Equilibria*, 3rd ed.; Prentice Hall: New Jersey, 1999.
(24) Gromov, D. G.; Pablo, J. J.; Luna-Bárcenas, G.; Sanchez, I. C.; Johnston, K. P. *J. Chem. Phys.* **1998**, *108*, 4647.
(25) Hino, T.; Prausnitz, J. M. *Macromolecules* **1998**, *31*, 2636.
(26) Ruzette, A. V. G.; Mayes, A. M. *Macromolecules* **2001**, *34*, 1894.
(27) (a) Dudowicz, J.; Freed, K. F. *Macromolecules* **1991**, *24*, 5076. (b) Dudowicz, J.; Freed, K. F.; Douglas, J. F. *Phys. Rev. Lett.* **2002**, *88*, 095503. (c) Dudowicz, J.; Freed, K. F. *Macromolecules* **1993**, *26*, 213.
(28) Cho, J. *Macromolecules* **2004**, *37*, 10101; Cho, J.; Kwon, Y. K. *J. Polym. Sci., Polym. Phys. Ed.* **2003**, *41*, 1889.
(29) Hseih, D. T.; Peiffer, D. G.; Rabeony, M.; Siakali-kioulafa, E.; Hadjichristidis, N. *Macromolecules* **1993**, *26*, 4978.
(30) Beiner, M.; Huth, H. *Nat. Mater*. **2003**, *2*, 595.
(31) Hiller, S.; Pascui1, O.; Budde, H.; Kabisch1, O. Reichert, D.; Beiner, M. *New J. Phys.* **2004**, *6*, 10.
(32) Colthup, N. B.; Daly, L. H.; Wiberley, S. E. *Introduction to Infrared and Raman Spectroscopy*, 3rd ed.; Academic Press: San Diego, CA, 1990; Chapter 8, pp 261−281.